Nonlinear protein degradation and the function of genetic circuits

Nicolas E. Buchler[†‡], Ulrich Gerland[§], and Terence Hwa[¶]

[†]Center for Studies in Physics and Biology, The Rockefeller University, New York, NY 10021; [§]Physics Department and Center for Nanoscience, Ludwig-Maximilians University, 80539 Munich, Germany; and [¶]Physics Department and Center for Theoretical Biological Physics, University of California at San Diego, La Jolla, CA 92093-0374

Edited by Alexander Varshavsky, California Institute of Technology, Pasadena, CA, and approved May 6, 2005 (received for review December 21, 2004)

The functions of most genetic circuits require a sufficient degree of cooperativity in the circuit components. Although mechanisms of cooperativity have been studied most extensively in the context of transcriptional initiation control, cooperativity from other processes involved in the operation of the circuits can also play important roles. In this work, we examine a simple kinetic source of cooperativity stemming from the nonlinear degradation of multimeric proteins. Ample experimental evidence suggests that protein subunits can degrade less rapidly when associated in multimeric complexes, an effect we refer to as "cooperative stability." For dimeric transcription factors, this effect leads to a concentration-dependence in the degradation rate because monomers, which are predominant at low concentrations, will be more rapidly degraded. Thus, cooperative stability can effectively widen the accessible range of protein levels *in vivo*. Through theoretical analysis of two exemplary genetic circuits in bacteria, we show that such an increased range is important for the robust operation of genetic circuits as well as their evolvability. Our calculations demonstrate that a few-fold difference between the degradation rate of monomers and dimers can already enhance the function of these circuits substantially. We discuss molecular mechanisms of cooperative stability and their occurrence in natural or engineered systems. Our results suggest that cooperative stability needs to be considered explicitly and characterized quantitatively in any systematic experimental or theoretical study of gene circuits.

amplification | dimerization | bistability | oscillation

It is widely recognized that controlled proteolysis, where the degradation of one protein depends on the presence of another protein in the cell, can play an important regulatory role in genetic circuits (1). Here, we examine another effect of proteolysis that does not involve such regulatory control, but can nevertheless impact the function of genetic circuits in important ways. It is a kinetic, cooperative effect predicated on the following two essential ingredients: (*i*) the fact that many proteins perform their physiological functions as dimers or higher-order oligomers, and (*ii*) the tendency for the oligomers to be more stable (to proteolysis) than their monomeric components. This effect, referred to below as "cooperative stability," has been discussed previously in qualitative terms in the context of many well-studied examples in prokaryotes and eukaryotes (1, 2). For example, in the SOS response of *Escherichia coli*, UmuC degradation is rescued by oligomerization with $UmuD'_2$ (3). Additionally, in *Saccharomyces cerevisiae*, the dimerization of a1 and α2 reduced the degradation rate by as much as 15-fold (4). Possible molecular mechanisms that give rise to cooperative stability include enhanced thermal stability of proteins upon mutual association [because thermal instability correlates with the rate of degradation (5, 6)] and the burial of proteolytic recognition sequences between protein interfaces (4).

Although most of the previous studies of cooperative stability focused on protein complexes with heterogeneous protein subunits, we study here its effect for typical transcription factors (TFs) that exert their biological functions only as homodimers (7). For those proteins that are intended to be present at a "low" and a "high" concentration at two distinct states of the cell, we show that cooperative stability can help widen the ratio between the two protein concentrations *in vivo*, when compared with the ratio of the mRNA levels in the two states. This amplification effect follows simply from the nonlinear dependence of the protein degradation rate on the concentration, i.e., enhanced degradation rate at lower concentrations due to the predominance of monomers or, alternatively, the enhanced stability of dimers that are predominant at higher concentrations. Through theoretical analysis of two model gene circuits in bacteria, we will illustrate that cooperative stability can significantly enhance the function of these circuits. Specifically, we show that a several-fold effect in cooperative stability can make gene circuits more robust to stochastic fluctuations while broadening the basin of parameter space supporting the circuit function. The latter effect enhances the evolvability of the circuit.

Circuits and Models

We analyze two basic genetic circuits, one that displays bistability and the other spontaneous oscillation. Both are important classes of behavior in biomolecular circuits. The first circuit consists of only a single gene with a gene product that can activate its own transcription (see Fig. 1*a*). This bistable switch is one of the simplest circuits that can produce two stable states (at LOW and HIGH levels of transcriptional activities), as was shown by theoretical analysis and an experimental implementation in *E. coli* (8). The second circuit we analyze consists of three genes connected in a ring topology, each repressing the transcription of its downstream partner (see Fig. 1*b*). This "repressillator" has been shown to spontaneously oscillate, both theoretically and experimentally (9).

Rather than modeling these circuits in full detail, our goal here is to use these circuits to identify generic effects that cooperative stability can impart to their functions. Accordingly, we use simple quantitative models and describe each circuit by only a few essential parameters, so that the effects of cooperative stability can be made transparent. Fig. 2 summarizes the biochemical processes considered in our model together with the associated rates. We describe the net change in the mRNA concentration due to transcription and turnover by the simple rate equation

$$\frac{dm}{dt} = \alpha \cdot g([\mathrm{TF}]) - \lambda_m \cdot m, \qquad [1]$$

where α denotes the transcription rate of the promoter at full activation, $g([\mathrm{TF}])$ is the relative promoter activity as a function of the TF concentration [TF] (see Fig. 3), and λ_m is the

This paper was submitted directly (Track II) to the PNAS office.

Abbreviation: TF, transcription factor.

[‡]To whom correspondence should be addressed. E-mail: buchler@rockefeller.edu.

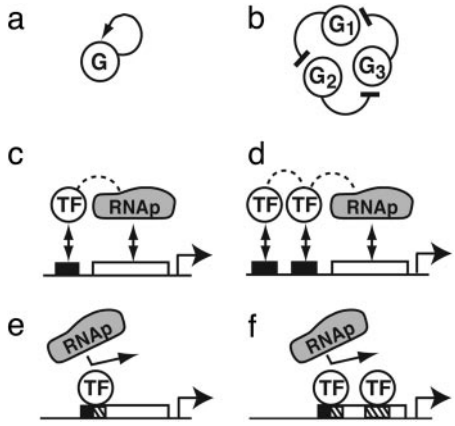

Fig. 1. Two simple genetic circuits. (*a* and *b*) The circuits shown are capable of bistability (*a*) and oscillation (*b*). Genetic circuits consist of genes (drawn as circles) that regulate the transcriptional activity of one another. This regulation can be activating (arrow) or repressive (blunt line). (*c–f*) Exemplary cis-regulatory architectures in bacteria by using one (*c*) or two (*d*) operator sites for activation and one (*e*) or two (*f*) operator sites for repression. The core promoter to which RNA polymerase (RNAp) binds and the operator sites to which the TFs bind are drawn as open or black boxes, respectively. The dashed lines depict cooperative interaction between regulatory proteins, whereas overlapping operators (indicated by hatched boxes) denote repression mediated through excluded volume interaction.

degradation rate of mRNA. Similarly, the net change in total protein concentration p is

$$\frac{dp}{dt} = \nu \cdot m - (\lambda_{p_1} \cdot p_1 + 2\lambda_{p_2} \cdot p_2), \qquad [2]$$

where ν denotes the translation rate of mRNA. In the turnover term, the total protein concentration $p = p_1 + 2p_2$ is partitioned into monomers and dimers with concentrations p_1 and p_2 and with turnover rates λ_{p_1} and λ_{p_2}, respectively. Note that the turnover term in Eq. **2** is linear in p when $\lambda_{p_1} = \lambda_{p_2}$ and becomes nonlinear in p with cooperative stability ($\lambda_{p_1} > \lambda_{p_2}$).

The protein products involved in our genetic circuits are all TFs, and as is often the case in bacteria, they function as activators or repressors only in the form of homodimers. Dimerization is assumed to be rapid, so that

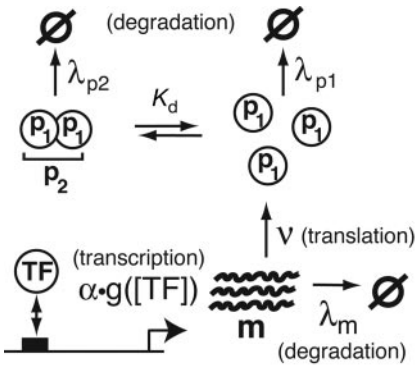

Fig. 2. Schematic of the basic parameters involved in transcription, translation, degradation, and dimerization. Transcription is governed by the transcription rate $\alpha \cdot g([TF])$, where α is the mRNA synthesis rate at full activation. Each mRNA is translated into protein monomer at a rate ν and degraded at a rate λ_m. The cellular concentrations of monomers (p_1) and dimers (p_2) are related by the dimer dissociation constant K_d. The protein degradation rate can be different for monomers (λ_{p_1}) and dimers (λ_{p_2}).

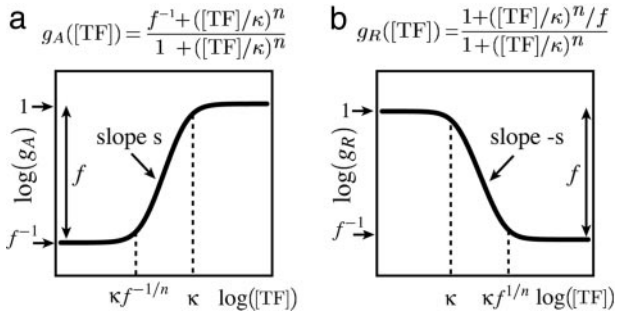

Fig. 3. Log–log plot of the relative promoter activity $g([TF])$ vs. the TF concentration [TF] for activation (*a*) and repression (*b*). The general expression for the promoter activity function is written above each plot. The peak activity of a promoter is defined to be 1, the fold-change between LOW and HIGH plateaus is described by f, and the DNA-binding dissociation constant of a TF for its operator (κ) is the concentration that separates the HIGH plateau from the transition region. The log–log slope (s) of the transition region [referred to as ''sensitivity'' or ''gain'' in the literature (10)] quantifies the degree of cooperativity in transcriptional control. It is determined by the Hill coefficient n and the maximum fold-change f, with maximum s approaching n for large f (see *Supporting Text*). Both *a* and *b* are approximations to promoter activity functions derived from the detailed thermodynamic treatment of transcriptional initiation (see *Supporting Text* and refs. 11–14).

$$p_2 = \frac{p_1^2}{K_d}, \qquad [3]$$

where K_d is the equilibrium dissociation constant.

In this work, we will not explicitly include the stochastic effects of transcription, translation, and dimerization. Stochastic fluctuations are dominant when the mRNA or protein concentrations are low (15–17). Nevertheless, our formulation in Eqs. **1–3** corresponds to the statistically averaged results of more complex models that do include these stochastic effects (18). The advantage of our approach is that it allows us to rapidly elucidate the average behavior of each circuit for all combinations of its parameters. By demanding that the average protein concentrations not be too small, we can identify those (desirable) combinations of parameters for which the circuit behavior is mostly insensitive to stochastic effects.

Results

For each circuit shown in Fig. 1 *a* and *b*, we want to identify the effect of cooperative stability on its function by using the quantitative model described above. Toward this end, we first determine the parameter regime where the circuit is operational (i.e., bistable or oscillatory) without cooperative stability ($\lambda_{p_1} = \lambda_{p_2}$) and then with cooperative stability ($\lambda_{p_1} > \lambda_{p_2}$). For the latter case, we make the (reasonable) assumption that dimer turnover occurs mainly by cell growth/dilution, whereas monomers can experience accelerated degradation. Thus, we take the typical half-life of dimers to be of the order of the cell-doubling time (≈50 min for bacteria in the exponential growth phase), whereas the typical half-life of monomers can be shortened to a few minutes. In this section, we present our results for the bistable circuit. The effect of cooperative stability on oscillation is equally striking; the detailed results are presented in *Supporting Text*, Table 2, and Figs. 5–12, which are published as supporting information on the PNAS web site.

Bistable Circuit. Because this circuit consists of a single gene with positive autoregulation, and only dimers can activate transcription, the promoter activity increases with the dimer concentration. This promoter activity function g_A is sketched in Fig. 3*a*,

Table 1. Physiological range of the model parameters

Parameter	Description	Typical *in vivo* values	Principal molecular determinants	Refs.
f	Maximum fold-change in promoter activity	10∼100 (activator) 10∼1000† (repressor)	Strength of TF–RNAp interaction	25, 27
n	Cooperativity in promoter activity	1∼2	Number of operator-bound TFs interacting with RNAp	28
κ	**TF-operator dissociation constant**	**1∼1,000 nM‡**	**Operator sequence**, binding interface of TF	19 and refs. therein
λ_m^{-1}	mRNA half-life	≈5 min		29
λ_p^{-1}	Protein half-life	≈50 min (dilution); approximately a few minutes (proteolysis)	Growth rate (dilution), protein stability, degradation tag (proteolysis)	1, 30
γ	**Protein synthesis rate at full activation**	**0∼100 nM/min§**	**Ribosome-binding site,** transcriptional efficiency	20, 31
K_d	Dimer dissociation constant	≈10 nM¶	Monomer–monomer affinity	21–24

Summary of the important parameters in our model together with their typical *in vivo* values in bacteria and the principal molecular properties that determine their values. The entries shown in boldface refer to those parameters that are programmable over a wide range; these programmable parameters play important roles in the natural evolution and synthetic design of promoters (12, 19). The last column lists exemplary references for the indicated physiological parameter range.

†Because repression involves TF–RNAp exclusion (a much stronger type of interaction than the weak attraction between RNAp and activators), the achievable fold changes in repression can readily be much larger, e.g., $f \sim 1000$.

‡The programmable parameter κ can be tuned by changing the number of bases matching the sequence for optimal TF-operator binding.

§Another programmable parameter is γ through choice of the ribosome-binding site (RBS). Maximum protein synthesis rate is limited by the rate of elongation of the ribosome. In bacteria, the elongation rate of ribosome is ≈20 codons/sec and ribosomes occlude ≈10 codons (31). Thus, the absolute maximum rate of protein synthesis per mRNA is ≈120 proteins per min. Typical genes in bacteria have on average approximately two mRNA per cell (29), so that even with an optimal RBS, the maximum γ is less than ≈240 nM/min. For proteins that are diluted through cell division (≈50 min), this range of γ produces steady-state protein concentrations of 0∼10,000 nM.

¶A number of bacterial TFs, e.g., BlaI (32), FIS (23), and CopR (33), have K_d in the micromolar range. However, they are all ''atypical'' regulatory proteins whose *in vivo* concentrations in the active state exceed the order of 10 μM (32–34). It is generally believed that the overexpression of many TFs can be deleterious to the cells. For example, the maximum concentration for typical TFs in bacteria is not much more than ≈100 nM; even the global regulator Crp is present only at ≈1,500 nM (35). Thus, typical bacterial TFs tend to be at lower concentrations *in vivo* and tend to have smaller K_d.

with $[TF] = p_2$. For any initial mRNA and protein concentration, this circuit will settle into a steady state given by the condition

$$\gamma \cdot g_A(p_2^*) = \lambda_{p_1} \cdot \sqrt{K_d p_2^*} + 2\lambda_{p_2} p_2^* \qquad [4]$$

where p_2^* denotes the steady-state dimer concentration, and $\gamma = \alpha \cdot \nu / \lambda_m$ is the protein synthesis rate of this gene at full activation. Eq. **4** is a simple statement that at steady state, the protein synthesis rate (left-hand side) must balance the total protein degradation rate (right-hand side).

Regime of bistability. Bistability results when Eq. **4** has two stable solutions for p_2^*, so that the gene can settle in either a HIGH or LOW state depending on the initial condition. This property depends on the parameters γ, K_d, and the λ_p values, as well as the shape of the promoter activity function $g_A(p_2)$. The latter function is characterized by the following three parameters (13, 14) as shown in Fig. 3*a*: (*i*) f, the fold change in promoter activity between the basal and fully activated levels; (*ii*) κ, the TF concentration where the promoter activity begins to saturate; and (*iii*) n, the effective Hill coefficient that describes the cooperativity of the promoter activity function. Among these parameters, κ and γ can easily be varied over several orders of magnitude by means of choice of the operator (19) and the ribosomal-binding sequences (20), respectively (we refer to these parameters as "programmable"). In contrast, the parameters f, n, and K_d tend to be more constrained physiologically. For example, although there is no intrinsic biochemical constraint for K_d to be small (see footnote ¶ in Table 1), values around $K_d \approx 10$ nM nevertheless appear to be typical according to *in vitro* measurements,‖ e.g., $K_d \approx 20$ nM for λCI (21), $K_d \approx 8$ nM for Arc (22), $K_d \approx 10$ nM for NtrC (23), and $K_d \approx 1$ nM for Crp (24). Similarly, the maximal fold-change f in activation, which reflects the strength of the interaction between the activator and the RNA polymerase (13, 14), is typically limited to the order of 10 ∼ 100 (25). Moreover, although there is no intrinsic difficulty in modifying the strength of the protein–protein interaction through natural or directed evolution (26), in practice f is not expected to be very programmable due to pleiotropy, because the modification of activator–polymerase interaction would simultaneously affect the expression of all genes controlled by the activator. Table 1 summarizes the physiological range for all of the parameters introduced in our model. Because our goal is to study the circuit behavior for typical physiological parameters, we will perform our analysis for a wide range of values in the programmable parameters κ and γ and only a few representative values of f, n, and K_d.

Since the bistability of the circuit depends only on certain combinations of the parameters (see *Supporting Text*), it is revealing to plot the regime of bistability as a function of the programmable parameters by using the combinations K_d/κ and $\gamma/(\kappa\lambda_{p_2})$ on the horizontal and vertical axes, respectively (see Fig. 4*a*). The remaining parameters are fixed at $n = 1$ and $f = 100$, which corresponds to a strong activator (e.g., Crp) with a single operator site as shown in Fig. 1*c*.

Circuit without cooperative stability. For $\lambda_{p_1} = \lambda_{p_2}$, the corresponding bistable regime is the narrow black strip at the lower right corner of Fig. 4*a*. For a given value of K_d, the black region defines an acceptable range of γ for each value of κ. The circuit behavior within the bistable regime is shown in Fig. 4*b* by plotting the steady-state monomer and dimer concentrations (gray and black curves, respectively) in the bistable HIGH and the LOW state (solid and dashed lines, respectively) as a function of κ, by using the typical dimer dissociation constant of $K_d = 10$ nM. Note that the steady-state TF concentrations are very low, not exceeding $p_2^* \sim 10$ nM, which corresponds to ≈10 molecules per bacterial cell. Such low concentrations are difficult to maintain reliably,

‖The effective value of K_d *in vivo* is expected to increase with respect to its *in vitro* value because of dimer turnover. The amount of increase depends on the dimer association and dissociation rates k_a and k_d. We find $K_d = (k_d + \lambda_{p2})/k_a$ instead of the usual *in vitro* expression $K_d = k_d/k_a$. However, for typical small proteins, this increase is estimated to be less than ≈1 nM and hence is not important for this discussion (see *Supporting Text*).

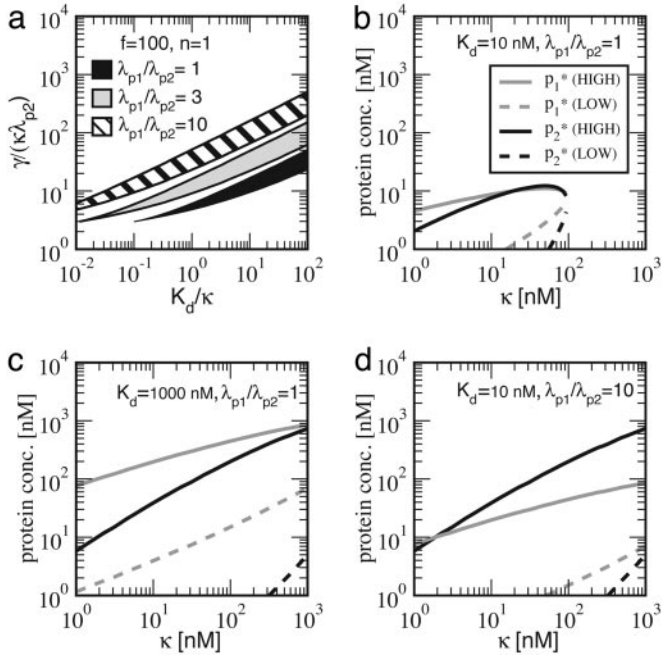

Fig. 4. Quantitative characteristics of the bistable circuit with a single operator promoter ($n = 1$) and a strong activator ($f = 100$). (*a*) Regime of bistability in the parameter space for the circuit with linear degradation ($\lambda_{p_1}/\lambda_{p_2} = 1$) and with cooperative stability ($\lambda_{p_1}/\lambda_{p_2} > 1$). The axes show combinations of the parameters that are both useful for discussion and natural in the quantitative description (see *Supporting Text*). (*b* and *c*) For linear degradation, the steady-state monomer (gray) and dimer (black) concentrations (i.e., p_1^* and p_2^*, respectively) are plotted for different values of κ, with $K_d = 10$ nM (*b*) and 1,000 nM (*c*). For each choice of K_d and κ, γ is chosen such that the system is in the middle of the bistable regime, i.e., the black band in *a*. For both p_1^* and p_2^*, the solid curve is the concentration in the HIGH bistable state and the dashed curve is the concentration in the LOW bistable state. (*d*) Same plot as *b* for the circuit with cooperative stability ($\lambda_{p_1}/\lambda_{p_2} = 10$).

and the circuit will be susceptible to various sources of stochastic fluctuations (36, 37). Similar results are obtained by using our model with $f = 11$ and $n \approx 1.7$, which mimics the bistable circuit studied experimentally by Isaacs *et al.* (8) (see Figs. 6 and 8). We note that strong fluctuations were indeed observed in that experiment.

The steady-state protein concentrations could be raised (consequently reducing stochastic effects) by increasing K_d, e.g., to $K_d = 1{,}000$ nM as shown in Fig. 4*c*. In this case, however, the concentration of the nonfunctional monomers (gray curves) is significantly larger than the concentration of functional dimers (black curves). Indeed, without cooperative stability, monomer overproduction is a generic consequence of leveraging cooperativity from dimerization because the system can only exploit this source of cooperativity when the total protein concentration is much less than K_d (i.e., when the protein exists primarily in monomer form). Although the overproduction of monomers may or may not be detrimental to the cell for an individual gene, the monomer "load" can become a significant problem if weak dimerization becomes a strategy widely adopted by the cell, e.g., if every regulatory gene contributes $10 \sim 100$ nonfunctional monomers in the LOW or HIGH states. This observation is a conceivable explanation for the small K_d values found for typical dimeric proteins.

Effect of cooperative stability. The gray and hatched areas in Fig. 4*a* show how the bistable parameter regime is shifted when cooperative stability is introduced with $\lambda_{p_1}/\lambda_{p_2} = 3$ and $\lambda_{p_1}/\lambda_{p_2} = 10$, respectively. For a given value of K_d, cooperative stability shifts the bistable regime toward an increased rate of protein synthesis γ. An elevated γ reduces the susceptibility of the bistable circuit to stochastic fluctuations by increasing the protein concentration. This increase is seen explicitly in Fig. 4*d*, where we again plot the steady-state monomer and dimer concentrations in the bistable HIGH and LOW states with the typical $K_d = 10$ nM as in Fig. 4*b* but with 10-fold cooperative stability ($\lambda_{p_1} = 10\lambda_{p_2}$). Comparison of Fig. 4 *d* and *c* demonstrates that cooperative stability also reduces the monomer load significantly.

Oscillatory Circuit. In general, oscillation is favored when the following characteristics apply: (*i*) the fold-change *f* is large, (*ii*) the protein monomer and mRNA turnover rates are comparable, and (*iii*) there is a large cooperativity/nonlinearity in synthesis and/or degradation (see *Supporting Text*). We study repressive promoters with a single operator site ($n = 1$; Fig. 1*e*). Our results (Fig. 10*a*) show that in the absence of cooperative stability ($\lambda_{p_1} = \lambda_{p_2}$), the system cannot sustain oscillations for typical $K_d = 10$ nM and typical $\kappa \sim 1$–$1{,}000$ nM. However, by introducing cooperative stability and destabilizing the monomers with respect to the dimer species ($\lambda_{p_1} > \lambda_{p_2}$), oscillation becomes possible with the parameter range of typical molecular components (see Fig. 10*b*).

Discussion

Benefits of Cooperative Stability. We examined the function of simple genetic circuits with dimeric TFs that exhibit different degrees of cooperative stability, where the turnover of monomers is more rapid than that of the functional dimers. In the absence of cooperative stability, the desired operation of both the one-gene switch and the three-gene oscillator requires parameters that are on the edge of what is physiologically realizable. These limitations can be understood in simple terms. Proper function of most biological circuits requires a sufficient degree of cooperativity in the circuit components. Cooperativity at the transcriptional initiation stage (controlled by the fold-change *f* and the Hill coefficient *n* in our model of transcriptional control) is usually quite limited. It is thus crucial to harness cooperativity from the other processes involved in the operation of gene circuits. A simple and direct source of cooperativity that does not involve additional genes and proteins is the nonlinearity in TF dimerization. To harness this source of nonlinearity, however, it is necessary to maintain the cellular TF level at or below the dimer dissociation constant K_d. This constraint leaves the system with two undesirable options. One option is to use typical dimeric TFs with $K_d \sim 10$ nM and maintain the TFs at a very low level (e.g., <10 molecules per cell); this option leaves the system vulnerable to stochastic fluctuations. The alternative is to maintain a higher TF level (e.g., ≈100 nM) to reduce these fluctuations. However, this alternative requires the use of TFs with large K_d that exposes the system to an increased load of nonfunctional monomers.

We have shown that cooperative stability removes the link between the cellular TF levels and the K_d values. Cooperative stability makes it possible to simultaneously maintain a cellular TF level that is robust to fluctuations while allowing the circuit to harness dimer cooperativity for the typical (strong) dimers; the latter property relieves the system of the monomer load problem. This benefit of cooperative stability stems from the fact that dimer cooperativity can be used as long as monomer degradation is the predominant degradative pathway ($\lambda_{p_1}:p_1 > 2\lambda_{p_2}:p_2$; see discussion below and *Supporting Text*). Thus, by increasing $\lambda_{p_1} > \lambda_{p_2}$, the *in vivo* concentration over which dimer cooperativity can be harnessed is extended (beyond the limit imposed by K_d).

From the perspective of gene expression, the effect of cooperative stability may be characterized as that of amplification, because it can produce a larger fold change in dimer expression compared with the fold change in mRNA expression. Consider the situation where monomer degradation much exceeds dimer

degradation ($\lambda_{p_1} \gg \lambda_{p_2}$). In this limit, an x-fold change in protein synthesis (due to an x-fold change in mRNA expression) must be balanced by the same x-fold change in monomer degradation in the steady state. The latter requires an x-fold change in monomer concentration, which implies an x^2-fold change in the dimer concentration due to the monomer–dimer equilibrium condition of Eq. **3**. Thus, the potential power of amplification derivable from cooperative stability is substantial and not limited by the value of K_d. Although we have not discussed higher-order oligomers, similar estimates show that an x-fold change in mRNA expression can result in up to an x^m-fold change in protein concentration for obligatory m-mers, making the power of amplification even larger and independent of the multimer dissociation constant.

We note that the effect of cooperative stability is independent of the function of the protein product itself. In particular, the protein multimer does not need to be a TF and can, for example, be an enzyme that is needed at a high level in one state and must be kept to a very low level in another state. Thus, cooperative stability can be a versatile and generic way to amplify the fold change in the expression of a large class of genes. However, cooperative stability has associated costs that should prevent its extensive usage: Because it relies on the active proteolysis of monomers, extensive use will saturate the proteolytic machinery in the cell. Similarly, a higher degradation rate would require a higher synthesis rate. However, because most of the increase in synthesis would be in the low state where monomers predominate, the increase in synthesis is not expected to be substantial (see *Supporting Text*).

Natural Occurrences of Cooperative Stability. How common is cooperative stability in cells, and how readily can cooperative stability be implemented (e.g., evolved) molecularly if the need arises? We already mentioned in the introduction a number of specific examples (1–6) where oligomerization provides protection against degradation. In these instances, the mechanisms of cooperative stability fell within the following two classes: (*i*) oligomerization enhances the thermal stability of the protein subunits, making them more resistant to proteolysis, and (*ii*) oligomerization buries the degradation tags that would have been exposed in monomeric subunits. However, most of the existing studies have been on heteromeric complexes. There has been a lack of focused systematic studies on state-dependent degradation of homodimers. One exception is the class of TFs mediating quorum-sensing pathways in bacteria. For example, the TF TraR is degraded within a few minutes in the monomeric form (in the absence of autoinducer) but becomes stabilized by at least 30-fold in the dimeric form in the presence of autoinducer (38). This big difference in degradation rates is attributed to major changes in the molecular structure between the monomers and dimers: TraR, like the other LuxR-family of TFs, is believed to be largely disordered (i.e., unfolded) in the monomeric form, becoming folded only upon dimerization in the presence of the autoinducer (39). The rapid monomer turnover then can be understood as a generic consequence of the rapid proteolysis of unfolded molecules in cells (5, 6).

It is currently unknown to what extent cooperative stability occurs for other TFs, many of which function as homodimers. However, the properties of the TraR system described above suggest that cooperative stability may occur generically if the monomers are unfolded. Here, we want to point out that there is in fact a large class of proteins (mostly regulatory proteins) that are natively unfolded, i.e., proteins that fold and are thermally stable only upon association with their targets (40). They include the so-called "two-state dimers" (41), an example of which is the Arc repressor of phage P22 (22). Conspicuous molecular features of the two-state dimers include the large number of intermonomer contacts (compared with intramonomer contacts) and the hydrophobicity of the interfacial contacts (42, 43). We conjecture that two-state dimers are ideal molecules to mediate cooperative stability, because unfolded monomers are generally more susceptible to generic degradation (5, 6), and their exposed hydrophobic surface patches are natural targets of various proteases (30). Spontaneous unfolding of monomers may be an elegant way by nature to keep the basal protein level low, while not disturbing the stable oligomers in the HIGH state.

Acquisition of Cooperative Stability. For the purpose of synthesizing robust genetic circuits in bioengineering applications (8, 9, 44–46), it will be useful to develop methods to endow a generic TF with cooperative stability. Such experiments would be useful for understanding how cooperative stability can arise over the course of natural evolution. A synthetic way of generating molecules with cooperative stability may have already been developed more than a decade ago: β-galactosidase molecules engineered with various N-end residues (obtained from *in vivo* N-terminal deletions) displayed non-first-order degradation kinetics in pulse-chase experiments (47). The authors already speculated that the slow degradation regime might correspond to the degradation of "matured" β-galactosidase tetramers that are more resistant to targeting and/or degradation by the N-end rule pathway (47). This finding is consistent with the idea that multimerization can stabilize a molecule by burying its degradation signal, in this case the unusual N-terminal residue according to the N-end rule (48). Systematic characterizations along the line of ref. 47 are clearly needed for a variety of molecules with various types of degradation tags, e.g., the N-end degrons (48) and C-terminal ssrA-tags (49). It is interesting to note that although ssrA-tags have been widely used to control protein turnover in synthetic genetic networks (9, 50, 51), the precise effect of ssrA-tags (e.g., whether they enhance the degradation of monomers and dimers equally and whether they preferentially enhance the degradation of monomers or dimers) has never been characterized. The occurrence of cooperative stability will depend on details of the protein structure, e.g., whether the C-terminal residues are buried in the interior of the protein complex.

In a different set of experiments (K. Plaxco, personal communication), stably folded proteins can become natively unfolded upon the deletion of a few residues at the peptide termini, and yet such proteins can still fold upon target presentation. The result is consistent with the expectation that peptide termini away from the interaction surface contribute toward the stability of the monomers but not the complex. If this result is generic for dimeric proteins and if unfolded molecules are rapidly degraded, then their degree of cooperative stability will be readily tunable by either synthetic molecular engineering or natural evolution.

Consequences for Circuit Modeling. Cooperative stability ($\lambda_{p_1} > \lambda_{p_2}$) has been included in the modeling of genetic circuits. For example, in *Drosophila*, reduced protein degradation by multimerization has been suggested to play a significant role in the genetic circuit controlling circadian rhythm (52, 53). Also, in modeling the phage λ's entry into lysogeny, Arkin *et al.* (54) assumed that CI monomers were degraded with a half-life of $\approx$15 min, and Cro monomers were degraded with a half-life of $\approx$5 min, while leaving the long-lived dimers to dilution by cell growth. With a cell-doubling time of $\approx$30–50 min, these assumptions implicitly invoke cooperative stability with $\lambda_{p_1}/\lambda_{p_2} \approx$ 2–3 for CI and $\lambda_{p_1}/\lambda_{p_2} \approx$ 6–10 for Cro.

In general, however, many models describing bistability or oscillation are often unintentionally locked into forms that assume either no cooperative stability (i.e., $\lambda_{p_1} = \lambda_{p_2}$) or extreme cooperative stability (i.e., $\lambda_{p_2} = 0$). For example, in their analysis of the robustness of phage λ's lysogenic phase (55), Aurell *et al.* (56) and Zhu *et al.* (57) assumed that monomers and dimers were

GENETICS

degraded with equal rates and concluded that additional source(s) of cooperativity are needed to explain the observed robustness. We suggest that cooperative stability might be another possible source of cooperativity that needs to be examined critically. In fact, it was speculated long ago (58) that concentration-dependent degradation of Cro (as suggested by the data in ref. 59) might provide some of the cooperativity needed to reconcile discrepancies between theory and experiment. Given the strong impact that even a modest degree of cooperative stability can make on the phase diagram and the circuit stability (see Fig. 4), knowledge of the monomer/dimer turnover rates is crucial to guide quantitative studies of the λ-switch and to help resolve puzzles regarding the stability and robustness of lysogeny. More generally, we hope our results will motivate the modeling community to be more attentive to protein degradation in future studies.

Evolutionary Aspects. As shown above, cooperative stability has broadened the parameter space for desired circuit operations. We suggest that this broadening of the operable parameter space is not only useful in relaxing the design constraints in synthetic biology experiments but may be important for such circuits to emerge from natural evolution: Evolvability of a circuit requires that before selection can exert any effect, it should be possible for the organism to spontaneously assemble a primitive circuit that can sustain some rudimentary operation conferring some limited fitness advantage. This possibility is enhanced if the circuit can operate by using components widely accessible to the cells. Of course, cooperative stability is not the only strategy to boost the degree of cooperativity needed for circuit operations. There exist alternative strategies that may provide stronger cooperativity, including nonlinear feedback at the level of transcriptional and translational initiation/termination as well as proteolytic control involving posttranslational modifications. However, such processes require additional genes and proteins. They may be the final outcome of extended refinement of genetic circuits through a prolonged evolutionary process. In contrast, cooperative stability does not require any additional molecular components except for the dimeric protein itself. Moreover, cooperative stability itself may be a readily evolvable molecular trait for typical dimeric proteins as just discussed above. Therefore, it may be used at early stages of evolution to provide a circuit with some rudimentary functions beneficial to the host, so that selection can begin to exert some effect.

We thank P. Ao, R. Bundschuh, J. J. Collins, F. R. Cross, J. Finke, R. Hampton, S. Leibler, K. Levy, M. Louis, K. Plaxco, M. Ptashne, J. Reinitz, R. Sauer, E. Siggia, J. Vilar, J. Widom, L. C. You, and M. W. Young for helpful comments. We especially thank W. F. Loomis for encouragement and suggestions throughout the course of this work. This work was initiated at the Center for Theoretical Biological Physics at the University of California at San Diego. N.E.B. was supported by a National Science Foundation bioinformatics fellowship. U.G. was supported by the Emmy Noether fellowship. T.H. was supported by a Burroughs–Wellcome functional genomics award and by National Science Foundation Grants 0211308, 0083704, 0216576, and 0225630.

1. Gottesman, S. & Maurizi, M. R. (1992) *Microbiol. Rev.* **56,** 592–621.
2. Jenal, U. & Hengge-Aronis, R. (2003) *Curr. Opin. Microbiol.* **6,** 163–172.
3. Gonzalez, M. & Woodgate, R. (2002) *BioEssays* **24,** 141–148.
4. Johnson, P. R., Swanson, R., Rakhilina, L. & Hochstrasser, M. (1998) *Cell* **94,** 217–227.
5. Parsell, D. A. & Sauer, R. T. (1989) *J. Biol. Chem.* **264,** 7590–7595.
6. Herman, C., Prakash, S., Lu, C. Z., Matouschek, A. & Gross, C. A. (2003) *Mol. Cell* **11,** 659–669.
7. Luscombe, N. M., Austin, S. A., Berman, H. M. & Thornton, J. M. (2000) *Genome Biol.* **1,** e001.1–e001.37.
8. Isaacs, F. J., Hasty, J., Cantor, C. R. & Collins, J. J. (2003) *Proc. Natl. Acad. Sci. USA* **100,** 7714–7719.
9. Elowitz, M. B. & Leibler, S. (2000) *Nature* **403,** 335–338.
10. Savageau, M. A. (1976) *Biochemical Systems Analysis: A Study of Function and Design in Molecular Biology* (Addison–Wesley, Reading, MA).
11. Shea, M. A. & Ackers, G. K. (1985) *J. Mol. Biol.* **181,** 211–230.
12. Buchler, N. E., Gerland, U. & Hwa, T. (2003) *Proc. Natl. Acad. Sci. USA* **100,** 5136–5141.
13. Bintu, L., Buchler, N. E., Garcia, H. G., Gerland, U., Hwa., T., Kondev, J. & Phillips, R. (2005) *Curr. Opin. Genet. Dev.* **15,** 116–124.
14. Bintu, L., Buchler, N. E., Garcia, H. G., Gerland, U., Hwa., T., Kondev, J., Kuhlman, T. & Phillips, R. (2005) *Curr. Opin. Genet. Dev.* **15,** 125–135.
15. McAdams, H. H. & Arkin, A. (1997) *Proc. Natl. Acad. Sci. USA* **94,** 814–819.
16. Thattai, M. & van Oudenaarden, A. (2001) *Proc. Natl. Acad. Sci. USA* **98,** 8614–8619.
17. Kepler, T. B. & Elston, T. C. (2001) *Biophys. J.* **81,** 3116–3136.
18. Bundschuh, R., Hayot, F. & Jayaprakash, C. (2003) *J. Theor. Biol.* **220,** 261–269.
19. Gerland, U., Moroz, J. D. & Hwa, T. (2002) *Proc. Natl. Acad. Sci. USA* **99,** 12015–12020.
20. de Smit, M. H. & van Duin, J. (1994) *J. Mol. Biol.* **244,** 144–150.
21. Sauer, R. T. (1979) Ph.D. thesis (Harvard Univ., Cambridge, MA).
22. Milla, M. E., Brown, B. M. & Sauer, R. T. (1994) *Nat. Struct. Biol.* **1,** 518–523.
23. Hobart, S. A., Ilin, S., Moriarty, D. F., Osuna, R. & Colon, W. (2002) *Protein Sci.* **11,** 1671–1680.
24. Harman, J. G. (2001) *Biochim. Biophys. Acta* **1547,** 1–17.
25. Ptashne, M. & Gann, A. (2001) *Genes & Signals* (Cold Spring Harbor Lab. Press, Woodbury, NY).
26. Yokobayashi, Y., Weiss, R. & Arnold, F. H. (2002) *Proc. Natl. Acad. Sci. USA* **99,** 16587–16591.
27. Lutz, R. & Bujard, H. (1997) *Nucleic Acids Res.* **25,** 1203–1210.
28. Wolf, D. M. & Eeckman, F. H. (1998) *J. Theor. Biol.* **195,** 167–186.
29. Bernstein, J. A., Khodursky, A. B., Lin, P. H., Lin-Chao, S. & Cohen, S. N. (2002) *Proc. Natl. Acad. Sci. USA* **99,** 9697–9702.
30. Wickner, S., Maurizi, M. R. & Gottesman, S. (1999) *Science* **286,** 1888–1893.
31. Alberts, B., Johnson, A., Lewis, J., Raff, M., Roberts, K. & Walter, P. (2002) *Molecular Biology of the Cell* (Garland, New York).
32. Filee, P., Vreuls, C., Herman, R., Thamm, I., Aerts, T., De Deyn, P. P., Frere, J. M. & Joris, B. (2003) *J. Biol. Chem.* **278,** 16482–16487.
33. Steinmetzer, K., Hillisch, A., Behlke, J. & Brantl, S. (2000) *Proteins* **39,** 408–416.
34. Ali Azam, T., Iwata, A., Nishimura, A., Ueda, S. & Ishihama, A. (1999) *J. Bacteriol.* **181,** 6361–6370.
35. Cossart, P. & Gicquel-Sanzey, B. (1985) *J. Bacteriol.* **161,** 454–457.
36. Elowitz, M. B., Levine, A. J., Siggia, E. D. & Swain, P. S. (2002) *Science* **297,** 1183–1186.
37. Ozbudak, E. M., Thattai, M., Kurtser, I., Grossman, A. D. & van Oudenaarden, A. (2002) *Nat. Genet.* **31,** 69–73.
38. Zhu, J. & Winans, S. C. (2001) *Proc. Natl. Acad. Sci. USA* **98,** 1507–1512.
39. Vannini, A., Volpari, C., Gargioli, C., Muraglia, E., Cortese, R., De Francesco, R., Neddermann, P. & Marco S. D. (2002) *EMBO J.* **21,** 4393–4401.
40. Wright, P. E. & Dyson, H. J. (1999) *J. Mol. Biol.* **293,** 321–331.
41. Neet, K. E. & Timm, D. E. (1994) *Protein Sci.* **3,** 2167–2174.
42. Gunasekaran, K., Tsai, C.-J. & Nussinov, R. (2004) *J. Mol. Biol.* **341,** 1327–1341.
43. Levy, Y., Wolynes, P. G. & Onuchic, J. N. (2004) *Proc. Natl. Acad. Sci. USA* **101,** 511–516.
44. Gardner, T. S., Cantor, C. R. & Collins, J. J. (2000) *Nature* **403,** 339–342.
45. Becskei, A. & Serrano, L. (2000) *Nature* **405,** 590–593.
46. Atkinson, M. R., Savageau, M. A., Myers, J. T. & Ninfa, A. J. (2003) *Cell* **113,** 597–607.
47. Baker, R. T. & Varshavsky, A. (1991) *Proc. Natl. Acad. Sci. USA* **88,** 1090–1094.
48. Varshavsky, A. (1996) *Proc. Natl. Acad. Sci. USA* **93,** 12142–12149.
49. Gottesman, S., Roche, E., Zhoue, Y. & Sauer, R. T. (1998) *Genes Dev.* **12,** 1338–1347.
50. Guet, C. C., Elowitz, M. B., Hsing, W. & Leibler, S. (2002) *Science* **296,** 1466–1470.
51. Basu, S., Mehreja, R., Thiberge, S., Chen, M. T. & Weiss, R. (2004) *Proc. Natl. Acad. Sci. USA* **101,** 6355–6360.
52. Kloss, B., Price, J. L., Saez, L., Blau, J., Rothenfluh, A., Wesley, C. S. & Young, M. W. (1998) *Cell* **94,** 97–107.
53. Tyson, J. J., Hong, C. I., Thron, C. D. & Novak, B. (1999) *Biophys. J.* **77,** 2411–2417.
54. Arkin, A., Ross, J. & McAdams, H. H. (1998) *Genetics* **149,** 1633–1648.
55. Little, J. W., Shepley, W. P. & Wert, D. W. (1999) *EMBO J.* **18,** 4299–4307.
56. Aurell, E., Brown, S. Johanson, J. & Sneppen, K. (2002) *Phys. Rev. E Stat. Phys. Plasmas Fluids Relat. Interdiscip. Top.* **65,** 051914.
57. Zhu, X.-M., Yin, L., Hood, L. & Ao, P. (2004) *J. Bioinform. Comput. Biol.* **2,** 785–817.
58. Reinitz, J. & Vaisnys, J. R. (1990) *J. Theor. Biol.* **145,** 295–318.
59. Pakula, A. A. & Sauer, R. T. (1989) *Proteins* **5,** 202–210.